Flow Characteristics in HyperVapotron Elements Operating with Nanofluids

A. Sergis[1.1*], Y. Hardalupas[1.2] and T. R. Barrett[2]

[1]The Department of Mechanical Engineering, Imperial College London, London SW7 2AZ, UK
[2]EURATOM/CCFE, Culham Science Centre, Abingdon, Oxfordshire, OX14 3DB, UK
* E-mail: a.sergis09@imperial.ac.uk

Abstract: HyperVapotrons are highly robust and efficient heat exchangers able to transfer high heat fluxes of the order of 10-20MW/m^2. They employ the Vapotron effect, a complex two phase heat transfer mechanism, which is strongly linked to the hydrodynamic structures present in the coolant flow inside the devices. HyperVapotrons are currently tested in the Joined European Torus (JET) and the Mega Amp Spherical Tokamak (MAST) fusion experiments and are considered a strong candidate for the International Thermonuclear Experimental Reactor (ITER). The efficiency of heat transfer and the reliability of the components of a fusion power plant are important factors to ensure its longevity and economical sustainability. Optimisation of the heat transfer performance of these devices by the use of nanofluids is investigated in this paper. Nanofluids are advanced two phase coolants that exhibit heat transfer augmentation phenomena. A cold isothermal nanofluid flow is established inside two HyperVapotron models representing the geometries used at JET and MAST. A hybrid particle image velocimetry method is then employed to map in high spatial resolution (30μm) the flow fields inside each replica. The instantaneous and mean flow structures of a nanofluid are compared to those present during the use of a traditional coolant (water) in order to detect any departure from the hydrodynamic design operational regime of the device. It was discovered that the flow field of the JET model is considerably affected when using nanofluids, while the flow in the MAST geometry does not change significantly by the introduction of nanofluids. Evidence of a shear thinning mechanism is found inside the momentum boundary layer of the nanofluid flows and it might be important to calculating the pumping power losses of a functional nuclear fusion power plant cooling system ran with nanofluids instead of water. This work is a continuation of a previous study on HyperVapotrons and nanofluids, as documented by [1-3].

1. Introduction

HyperVapotrons (HV) are durable, reliable and high efficiency high heat flux (HHF) devices employing a cyclic phase change phenomenon to convey large heat fluxes (of the order of 10-20MW/m^2). They have been developed during the 50s for cooling klystron tubes however; the technology re-emerged recently as their capabilities make them good candidates as plasma facing components (PFC) in future fusion reactors. HV devices have been used on current experimental fusion reactors in the UK including JET. The physical heat transfer phenomenon employed by HVs (Vapotron effect) is complex and not well understood. Flow structures of coolant inside the device are expected to control their thermal performance [4-6]. An earlier study [3] provided high spatial resolution maps of the coolant flow structures inside two geometries (current HV geometries used in the JET and MAST devices) in isothermal conditions with water.

Efficient heat management is crucial to the overall fusion program viability. Along with traditional ways of optimisation of HV devices, we propose an additional option of further optimisation of HVs by re-designing their inner coolant flow and its thermal properties through the use of nanofluids. Nanofluids are binary mixtures of a solid and a carrier fluid (traditional coolants). The solids are usually below 100nm in size and in very small concentrations (<10% vol.). The technology was firstly envisaged by Choi in 1993 [7] and became a relatively popular topic during the last 16 years. This is due to the yet unexplained and dramatic heat transfer augmentation phenomena they exhibit [8-20]. Via statistical analysis of the literature [1] it was possible to quantify qualitatively the expected augmentation for the critical heat flux (CHF)

heat transfer mode up to 100-200% which is of particular interest for HHF applications such as nuclear fusion.

A cold isothermal high spatial resolution particle image velocimetry (PIV) experiment revealing the instantaneous and mean flow structures of a nanofluid flowing inside two HV models was performed. A comparison with the usual coolant (water) was subsequently performed to detect possible nanoparticle effects of the measured flow structures [3]. Calculation of the flow field is not possible via a computational fluid dynamic (CFD) simulations as proved by an earlier study [21] hence at this stage an experimental process is the only means of obtaining this type of measurements. An in depth image recognition routine was developed to process the PIV data and the geometrical features of the coolant flow observed in this study.

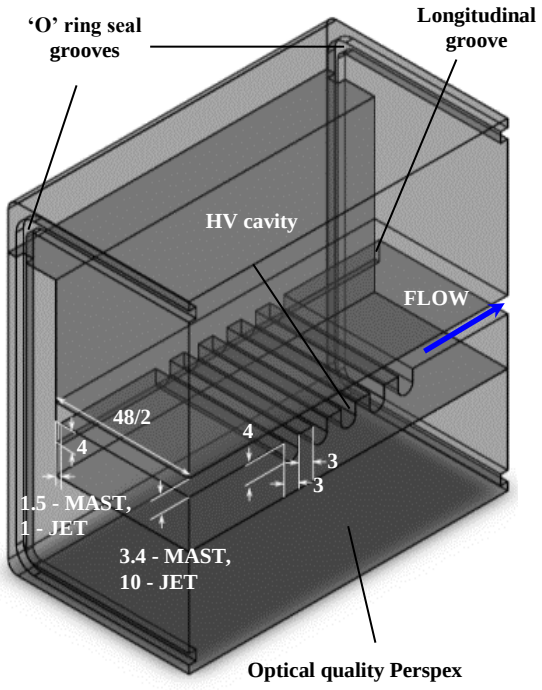

FIG. 1**.** Dimensionalised centre-line sectional view of the HV test sections under consideration. Dimensions are in mm.

2. Methodology

2.1. Experimental Apparatus

Two shortened HV variants from the JET and MAST experiments were manufactured from high optical quality transparent Perspex and used for the PIV experiment. The same models have also been used for an earlier study performed with water [3] (see FIG. 1 for a cut out). A closed circuit loop rig was developed to circulate the working fluid in each mock-up (same as the one used at [2, 3]). The free stream channel speed investigated was at 6m/s which is the nominal one used for experiments taking place at the Culham Centre for Fusion Energy (CCFE).

2.2. Instrumentation and Data Processing

The nanofluid was prepared by mixing Al_2O_3 dry particles of 50nm in diameter with water and subsequently ultrasonicating the mixture for 5 hours to break off any remaining agglomerates in the solution. The particle loading used was 0.0001%vol, which was the maximum allowable for PIV investigations [2]. PIV was employed to measure the flow via tracing/seeding particles (1μm Al_2O_3) and a type of photography using a laser as an illumination source (PIV). A hybrid method was employed for the nanofluid study, where the 'seeding' particles were mixed in the nanofluid [22]. Raleigh scattering from the nanoparticles added noise to the scattered light signal from the 'seeding' particles hence a very dilute nanofluid was used to allow for the methodology to work [2]. A 532nm wavelength Nd-Yag pulsed laser (Litron Nano T PIV) was used as an illumination source [3] with variable inter pulse time according to the expected flow velocities. A non-intensified LaVision Imager Intense CCD camera with a resolution of 1376x1040 pixels was used to capture the images. A Nikkor 50mm F/2.8 lens with manual focus was attached to the camera with a fitted band pass optical filter (10nm bandwidth around the 532nm wavelength) to reduce optical noise. The laser pulse pairs are emitted at a rate of 1Hz. The real area size captured by the camera is 35.6x26.9mm at a spatial resolution of 30μm. LaVision DaVis 7.2 software is used to record

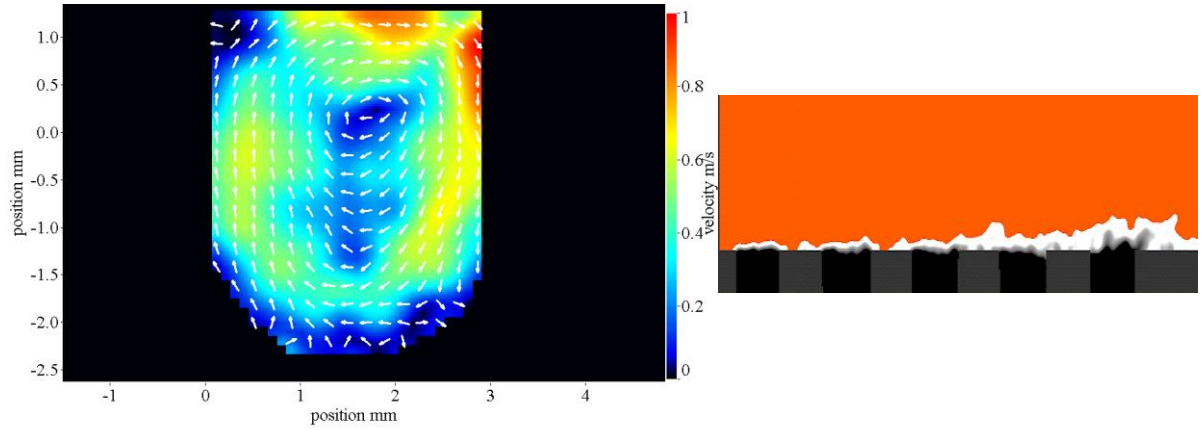

FIG. 2. Instantaneous example image of the velocity vector field inside the middle groove identifying a vortical structure (on the left) and a view of the entire test section with the wake formation highlighted in the free stream on top of the grooves (on the right). The white highlighted region in the right hand side image represents the velocity field region where the velocity magnitude is less than the bulk average of the free stream region.

and analyse the images. Shift and intensity correction is applied to the images followed by a multi pass cross correlation method to extract the initial velocity profile with the interrogation window dimensions ranging from 512x512 pixels down to 8x8 pixels with an overlap of 50%. Multi pass post processing was subsequently performed to improve the initial noisy calculated profile followed by additionally three filtering routines (cross correlation function peak ratio threshold filtering, median filtering and finally a smoothing filter is applied). The vector field calculations from each image pair to the next can are statistically independent. A total of 1000 image pairs were collected in each set of measurements which led to maximum statistical uncertainties of the order of ±3.8% and ±3.5% for the mean of JET and MAST respectively within a 95% confidence level. The maximum uncertainty of the measurements taking into account the PIV and flow meter uncertainty is hence estimated to be around 6% of the given quantities. Proper Orthogonal Decomposition and image recognition routines are used to post process the velocity data [3].

3. Results and Discussion

The focus of this study was the middle groove of the HV geometries used. Performance parameters such as time-averaged velocity vector maps, RMS of velocity fluctuations, singular groove flow comparison values for the velocity vector maps averaged in time and space (temporal and spatial averaging) are used to describe the vortex formation. The POD analysis makes apparent any significant out of the mean instantaneous flow structures that are smoothed out by the temporal averaging processes. Image recognition routines provide details regarding the instantaneous morphological behaviour of the vortex formation process which might be significant in defining the thermal performance of the device.

The results are non-dimensionalised by the target free stream speed for each condition. The spatial resolution of the velocity results was 30μm, while the uncertainty of the analysis for the characterisation of the vortex location was below ±500μm [3]. An instantaneous vortex centre location is considered to be high or low if it is more or less than 500μm away from average vortex centroid location for the particular groove and working condition. The analysis is one-dimensional and in the vertical dimension as indicated in *FIG.* 2. The POD analysis focused on the first four Eigen modes of the decomposition, since subsequent modes are less energetic or/and provide no additional information regarding the observed flow patterns. Similarly to

water, the first 5-10 POD modes carried most energy with the first four providing meaningful out of the mean structures in most cases [3].

The image recognition analysis resolves the state and centroid location of the instantaneous vortex formation (for example left hand side of *FIG.* 2). A flow analysis of the generated wakes from the grooves was also employed and took into account the instantaneous flow field inside the entire test section (for example right hand side of *FIG.* 2).

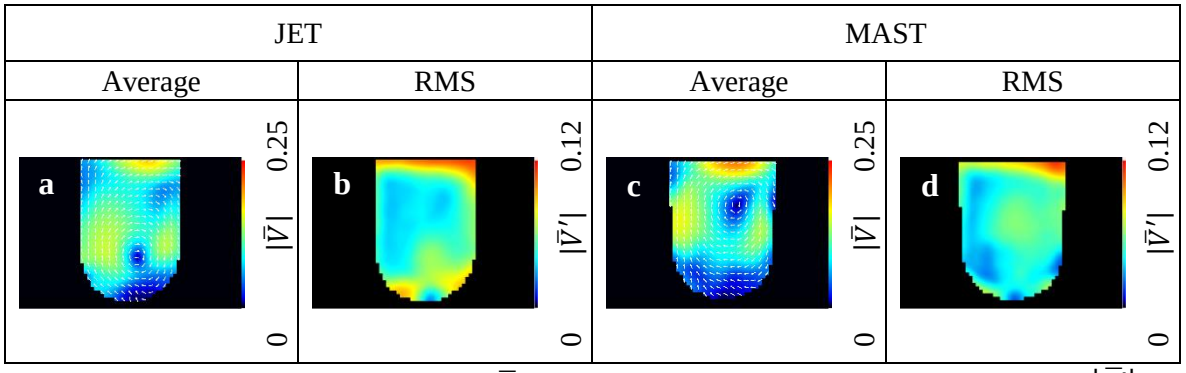

FIG. 3. Mean normalised velocity $\langle|\bar{\boldsymbol{V}}|\rangle$ and RMS of normalised velocity fluctuations $\langle|\bar{\boldsymbol{V}}'|\rangle$ for nanofluid flow in the JET and MAST geometries.

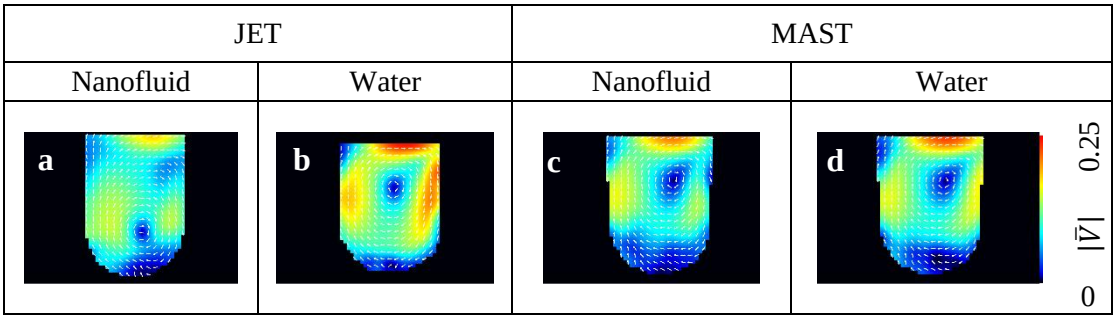

FIG. 4. Comparison of mean normalised velocity $\langle|\bar{V}|\rangle$ for nanofluid and water flow in the JET and MAST geometries.

Table I. Measured normalised speed characteristics with a water based nanofluid ($\langle|\bar{V}|\rangle$: Groove spatially averaged normalised speed, $\langle|\bar{V}'|\rangle$: Groove spatially averaged RMS of normalised velocity fluctuations, $\langle|\overline{V_{REL}}'|\rangle$: Groove spatially averaged RMS of normalised velocity fluctuations further normalised by $\langle|\bar{V}|\rangle$).

JET				MAST			
$\langle\|\bar{V}\|\rangle$	$\langle\|\bar{V}'\|\rangle$	$\langle\|\overline{V_{REL}}'\|\rangle$ / %	Vortex Breakup / %	$\langle\|\bar{V}\|\rangle$	$\langle\|\bar{V}'\|\rangle$	$\langle\|\overline{V_{REL}}'\|\rangle$ / %	Vortex Breakup / %
0.092792	0.052946	57.1	19.6	0.087924	0.047561	54.1	6.2

Table II. Comparison of measured normalised speed characteristics with a water based nanofluid and current operating conditions with water given as percentage changes. The maximum comparison uncertainty of the measurements is 6% hence any value smaller than that is considered uncertain up to the maximum uncertainty of 6%.

JET				MAST			
$\Delta\langle\|\bar{V}\|\rangle$ / %	$\Delta\langle\|\bar{V}'\|\rangle$ / %	$\Delta\langle\|\overline{V_{REL}}'\|\rangle$ / %	ΔVortex Breakup / %	$\Delta\langle\|\bar{V}\|\rangle$ / %	$\Delta\langle\|\bar{V}'\|\rangle$ / %	$\Delta\langle\|\overline{V_{REL}}'\|\rangle$ / %	ΔVortex Breakup / %
-24.0	26.5	22.8	17.2	-7.3	-1.1	3.4	-0.8

The normalised tabular data for the velocity field and breakup occurrences of the vortical formation inside the middle groove with the nanofluid can be found in Table I and their comparison with water can be found in Table II. A PIV visualisation is found in *FIG.* 3 and a comparison of the mean normalised velocity of the dilute nanofluid with water can be found in *FIG.* 4.

The average non-dimensional (ND) groove speed is decreased in both geometries via the use of a nanofluid (most significant decrease for the JET geometry). The RMS of the fluctuations for JET increases significantly whilst for the MAST geometry it presents a slight decrease. The relative RMS of velocity fluctuations for JET also increases significantly whilst for the MAST they remain about the same. The occurrences of the vortex break up are higher with the nanofluid in JET but remain unchanged for the MAST geometry. Morphologically, the vortex formation in the JET changes significantly (appears to form significantly lower inside the groove) whilst for MAST this remains unchanged. The significant change of the behaviour observed might be attributed to a viscosity change mechanism which appears more dominant due to the geometrical characteristics of the JET geometry.

The first four most energetic Eigen modes for both geometries were analysed. Unlike the corresponding POD analysis for the operation of JET with water [3], no distinctive out of the mean structures are found with a nanofluid in this geometry. The POD for the MAST geometry is similar between water and nanofluid operation indicating no significant departure from nominal operation unlike the JET case. Perhaps this behaviour might be a result of a fluid viscosity changing mechanism which becomes critical for the JET geometry but insignificant for the MAST geometry.

The vortex centroid is stabilised around its temporal average equilibrium position for the JET geometry with a probability of 62%-81% when nanofluids are used. This is significantly lower compared to the equivalent operation with water [3]). The JET geometry seems once more to deviate from its designed operation with the use of the dilute nanofluid whilst no significant deviation is found for the MAST geometry. The wake size and probability of occurrence reduced when using a nanofluid for the JET geometry compared to water conditions. No wake is detected for the MAST geometry either by using water or a dilute nanofluid.

It is not clear yet what causes the severe and repeatable operational deviations of the JET geometry when the dilute nanofluid is used instead of water whilst no change is observed in the operation of the MAST geometry. According to classical equations for micron sized slurries applied to nanofluids; the effective change of viscosity in the particular dilute nanofluid used is calculated to 2.5×10^{-4}% according to equation 1 (Einstein's effective viscosity equation derived for spherical micron sized suspensions [23]).

$$\mu_{eff} = (1 + 2.5\Phi)\mu_{BF} \quad (1)$$

where,
μbf : basefluid (water) viscosity
μeff : effective viscosity
Φ : nanoparticle volumetric concentration (0.0001% in this study)

This calculated change should not have been observed in this investigation; yet a significant deviation of the flow is observed which is many orders of magnitude larger than what classical thermodynamics dictates. The change in this study seems to be also geometry dependent which

leads us to believe that it might be associated with the momentum boundary layer formation near the walls of the JET geometry since all other operational conditions are kept constant in this experiment. The notion of an effective and anomalous change in the effective viscosity of nanofluids is also confirmed by other researchers in the literature however; it cannot be physically described using classical thermodynamics [24, 25]. This is the first time that the macroscopic effects of this mysterious phenomenon are revealed through PIV.

Viscosity change phenomena are of high importance in calculating the operational costs of any large scale water cooled system for the purpose of power generation as a significant amount of the produced energy is required to compensate for the pumping losses occurring when circulating the corresponding coolant through the plant. The effective viscosity phenomena observed through this work will dictate, perhaps up to a large degree, whether the expected beneficial heat transfer effects of nanofluids to be either counteracted or complimented by any change of the pumping energy losses involved. As such, further experimental research focusing on this aspect with various operational flow regimes in HVs with water and nanofluids should be carried out to observe the behaviour of this phenomenon better and seek a plausible explanation of its origin.

Finally, any possible effects of erosion have not been taken into account in this research and these should also be investigated to quantify the longevity and maintenance costs required to keep a nanofluid cooling circuit running for prolonged intervals (a study to take account of these effects is under way [26]).

4. Conclusions

Nanofluids are binary mixtures of a carrier fluid (traditional coolants) with very small concentrations of dispersed nano-sized particles. These mixtures have proven to potentially exhibit substantial thermal performance benefits over their carrier fluids which cannot be explained using classical thermodynamics. As such, nanofluids are investigated as potential candidates for HVs (a popular water cooled heat exchanger proposed for future nuclear fusion reactors) which might augment their overall thermal performance. Improvement of the heat handling processes will have a significant benefit on the overall efficiency and operational costs of future nuclear fusion power plants.

A cold isothermal investigation was performed in two transparent HV geometries similar to those used on the JET and MAST experiments in this study. The coolant structures established inside HVs are expected to control their thermal performance. A hybrid PIV method was able to map in high spatial resolution (30μm) the velocity vectors of coolants flowing inside the HV models. Water is the usual medium used inside HV devices. In this investigation, a nanofluid was used instead of water in order to investigate any departure of the device from its nominal operational regime. This hence deduces whether nanofluids might be beneficial or detrimental to the operation of HVs from a hydrodynamic point of view.

The investigation was performed with a dilute nanofluid (0.0001% vol.). It was discovered that the nanofluid had severely impacted the nominal flow structures in the JET geometry whilst it had no significant effect on the MAST geometry. The reason for this might be an effective viscosity change mechanism that affects the momentum boundary layers of the flow for the JET geometry. This is the first time the macroscopic effects of this phenomenon to have been observed through PIV in HVs and cannot be explained using classical thermodynamics. The effective viscosity variation might prove beneficial or detrimental to the overall pumping power losses of large scale cooling systems hence these must be further examined.

This work has been an attempt to model two HV geometries and understand their complex operation with nanofluids under simple boundary conditions. As such, the complex phase change phenomena employed by HVs when a heat flux is applied need to be further examined with nanofluids as their intricacy makes them hard to comprehend. The work is complimentary to previous studies performed with HVs [2, 3].

5. Acknowledgements

This work was funded by the RCUK Energy Programme and EURATOM. The views and opinions expressed herein do not necessarily reflect those of the European Commission.

6. References

1. Sergis, A. and Y. Hardalupas, *Anomalous heat transfer modes of nanofluids: a review based on statistical analysis.* Nanoscale Res Lett, 2011. **6**(1): p. 391.
2. Sergis, A., Y. Hardalupas, and T.R. Barrett, *Potential for improvement in high heat flux HyperVapotron element performance using nanofluids.* Nuclear Fusion, 2013. **53**(11).
3. Sergis, A., Y. Hardalupas, and T.R. Barrett, *Isothermal velocity measurements in two HyperVapotron geometries using Particle Image Velocimetry (PIV).* Experimental Thermal and Fluid Science, 2015. **61**: p. 48-58.
4. Pascal-Ribot, S., et al., *3D numerical simulations of hypervapotron cooling concept.* Fusion Engineering and Design, 2007. **82**(15-24): p. 1781-1785.
5. Escourbiac, F., *Experimental optimisation of a hypervapotron® concept for ITER plasma facing components.* Fusion Engineering and Design, 2003. **66-68**: p. 301-304.
6. Falter, H.D. and E. Thompson, *Performance of hypervapotron beam-stopping elements at JET.* Fusion Technology, 1996.
7. Das, S.K., et al., *Nanofluids*. First ed. 2007, Hoboken, NJ, USA: John Wiley & Sons, Inc.
8. Kim, H., et al., *On the quenching of steel and zircaloy spheres in water-based nanofluids with alumina, silica and diamond nanoparticles.* International Journal of Multiphase Flow, 2009. **35**(5): p. 427-438.
9. Rea, U., et al., *Laminar convective heat transfer and viscous pressure loss of alumina–water and zirconia–water nanofluids.* International Journal of Heat and Mass Transfer, 2009. **52**(7-8): p. 2042-2048.
10. Zhu, H., et al., *Preparation and thermal conductivity of CuO nanofluid via a wet chemical method.* Nanoscale Res Lett, 2011. **6**(1): p. 181.
11. Xuan, Y. and Z. Yao, *Lattice Boltzmann model for nanofluids.* Heat and Mass Transfer, 2004.
12. Xie, H., et al., *Nanofluids containing multiwalled carbon nanotubes and their enhanced thermal conductivities.* Journal of Applied Physics, 2003. **94**(8): p. 4967.
13. Wen, D., et al., *Review of nanofluids for heat transfer applications.* Particuology, 2009. **7**(2): p. 141-150.
14. Wen, D. and Y. Ding, *Experimental investigation into the pool boiling heat transfer of aqueous based γ-alumina nanofluids.* Journal of Nanoparticle Research, 2005. **7**(2-3): p. 265-274.
15. Wen, D., *Mechanisms of thermal nanofluids on enhanced critical heat flux (CHF).* International Journal of Heat and Mass Transfer, 2008. **51**(19-20): p. 4958-4965.
16. Wei, X., et al., *Synthesis and thermal conductivity of Cu2O nanofluids.* International Journal of Heat and Mass Transfer, 2009. **52**(19-20): p. 4371-4374.
17. Warrier, P. and A. Teja, *Effect of particle size on the thermal conductivity of nanofluids containing metallic nanoparticles.* Nanoscale Res Lett, 2011. **6**(1): p. 247.
18. Wang, X.-Q. and A.S. Mujumdar, *Heat transfer characteristics of nanofluids: a review.* International Journal of Thermal Sciences, 2007. **46**(1): p. 1-19.
19. Wang, X.B., et al., *Nanofluids in carbon nanotubes using supercritical CO2: a first step towards a nanochemical reaction.* Applied Physics A, 2003. **80**(3): p. 637-639.
20. Wang, G.-S. and R. Bao, *Two-phase flow patterns of nitrogen and nanofluids in a vertically capillary tube.* International Journal of Thermal Sciences, 2009. **48**(11): p. 2074-2079.

21. Sergis, A., et al., *Comparison of measurements and computations of isothermal flow velocity inside HyperVapotrons.* Fusion Engineering and Design, 2015.
22. Walsh, P.A., V.M. Egan, and E.J. Walsh, *Novel micro-PIV study enables a greater understanding of nanoparticle suspension flows: nanofluids.* Microfluidics and Nanofluidics, 2009. **8**(6): p. 837-842.
23. Einstein, A., *Eine neue Bestimmung der Moleküldimensionen.* Annalen der Physik, 1906. **324**(2): p. 289-306.
24. Buongiorno, J., *Convective Transport in Nanofluids.* Journal of Heat Transfer, 2006. **128**(3): p. 240-240.
25. Ding, Y., et al., *Heat transfer of aqueous suspensions of carbon nanotubes (CNT nanofluids).* International Journal of Heat and Mass Transfer, 2006. **49**(1-2): p. 240-250.
26. Barrett, T.R., et al., *Investigating the use of nanofluids to improve high heat flux cooling systems.* Fusion Engineering and Design, 2013. **88**(9-10): p. 2594-2597.